

# Structure of upper $g_{9/2}$ -shell nuclei and shape effect in the $^{94}\text{Ag}$ isomeric states

K. Kaneko,<sup>1,\*</sup> Y. Sun,<sup>2,3,†</sup> M. Hasegawa,<sup>4</sup> and T. Mizusaki<sup>5,6</sup>

<sup>1</sup>*Department of Physics, Kyushu Sangyo University, Fukuoka 813-8503, Japan*

<sup>2</sup>*Department of Physics, Shanghai Jiao Tong University, Shanghai 200240, P. R. China*

<sup>3</sup>*Joint Institute for Nuclear Astrophysics, University of Notre Dame, Indiana 46556, USA*

<sup>4</sup>*Institute of Modern Physics, Chinese Academy of Science, Lanzhou 730000, P. R. China*

<sup>5</sup>*Institute of Natural Sciences, Senshu University, Tokyo 101-8425, Japan*

<sup>6</sup>*Institut de Physique Nucléaire, Université Paris-Sud F-91406 Orsay CEDEX, France*

Using a shell model which is capable of describing the spectra of upper  $g_{9/2}$ -shell nuclei close to the  $N = Z$  line, we study the structure of two isomeric states  $7^+$  and  $21^+$  in the odd-odd  $N = Z$  nucleus  $^{94}\text{Ag}$ . It is found that both isomeric states exhibit a large collectivity. The  $7^+$  state is oblatelly deformed, and is suggested to be a shape isomer in nature. The  $21^+$  state becomes isomeric because of level inversion of the  $19^+$  and  $21^+$  states due to core excitations across the  $N = Z = 50$  shell gap. Calculation of spectroscopic quadrupole moment indicates clearly an enhancement in these states due to the core excitations. However, the present shell model calculation that produces the  $19^+ - 21^+$  level inversion cannot accept the large-deformation picture of Mukha *et al.* in Nature **439**, 298 (2006).

PACS numbers: 21.10.Dr, 21.60.Cs, 21.60.Jz, 21.10.Re

## I. INTRODUCTION

The structure study of  $N \approx Z$  nuclei is one of the current topics in nuclear physics. For the upper  $g_{9/2}$ -shell  $N \approx Z$  nuclei, perhaps the most interesting aspect is the occurrence of high-spin isomers. For decades, spin-gap isomers have been predicted by shell model calculations for nuclei close to the double-magic  $^{100}\text{Sn}$  [1]. Spin-gap isomers have recently been observed in some heavy  $N \approx Z$  nuclei, for example, in  $^{95}\text{Ag}$ ,  $^{95}\text{Pd}$ , and  $^{94}\text{Pd}$  [2]. From the shell model point of view, it is understood that these isomers are formed by an extra binding energy due to large attractive proton-neutron ( $pn$ ) interaction in the maximally aligned particle-particle or hole-hole configurations. Thus, one sensitive test for effective interactions in the shell model is a quantitative description of these high-spin states and their decay path.

The study of  $N \approx Z$  nuclei has important implications in nuclear astrophysics. It has been suggested that in x-ray binaries, nuclei are synthesized via the rapid proton capture process (rp process) [3, 4], a sequence of proton captures and  $\beta$  decays responsible for the burning of hydrogen into heavier elements. The rp process proceeds through the exotic mass region with  $N \approx Z$ . New reaction network calculations [5] have suggested that the rp process can extend up to the heavy Sn-Te mass region, involving the nuclei that we study in the present paper. Since the detailed reaction rates depend sensitively on the nuclear structure, information on energy levels of relevant nuclei is thus very useful. As emphasized by Schatz *et al.* [4], understanding the so-called waiting point nuclei is particularly important. Furthermore, if isomeric

states exist in the nuclei along the rp process path, the astrophysical significance [6, 7] could be that the proton capture on long-lived isomers may increase the reaction flow, thus reducing the timescale for the rp process nucleosynthesis during the cooling phase.

Because of the recent experimental successes, the high-spin  $I^\pi = 21^+$  and low-spin  $7^+$  isomers in the odd-odd  $N = Z$  nucleus  $^{94}\text{Ag}$  have become a discussion focus [8, 9, 10, 11]. In this nucleus, the high-spin  $21^+$  isomer has a high excitation energy of 6.7(5) MeV with a notably long half-life of 0.39(4) s, and is open to  $\beta$ , one-proton, and two-proton decays [12, 13]. Although the shell model calculations with the empirical effective interaction in the restricted ( $1p_{1/2}$ ,  $0g_{9/2}$ ) model space could reproduce the energy levels and high-spin isomers in  $^{95}\text{Ag}$ ,  $^{95}\text{Pd}$ , and  $^{94}\text{Pd}$ , it failed to predict the isomerism of  $21^+$  state in  $^{94}\text{Ag}$  [9, 10]. On the other hand, it has been shown that the large-scale shell model calculations with the extended model space ( $0g_{9/2}$ ,  $1d_{5/2}$ ,  $0g_{7/2}$ ,  $1d_{3/2}$ ,  $2s_{1/2}$ ) can obtain a  $21^+ - 19^+$  level inversion, which suggests that the core excitations across the  $^{100}\text{Sn}$  shell-closure play a crucial role in generating the  $21^+$  isomer with such a long half-life [9].

The analysis on one-proton decay [12] and two-proton decay [13] data of the  $21^+$  isomer in  $^{94}\text{Ag}$  has suggested a strong deformation picture for this state. The authors of Ref. [13] claimed that the unexpectedly large probability for the proton radioactivity could be attributed to a large deformation of the parent nucleus with a prolate shape. However, it is questionable that the  $21^+$  isomer in  $^{94}\text{Ag}$  is strongly deformed because the ground states of nuclei in this region are very weakly deformed. It has recently been pointed out [14] that the large-deformation claim remains a puzzle. On the other hand, the half-life of the low-spin  $7^+$  isomer has been measured to be 0.59(2) s [9], while the excitation energy is yet to be determined.

However, the question why these states become iso-

\*Electronic address: kaneko@ip.kyusan-u.ac.jp

†Electronic address: ysun@nd.edu, sunyang@sjtu.edu.cn

meric and what the nature of the isomerism is, has not been thoroughly addressed. Recently, we have investigated the structure of low-spin isomeric states in the odd-odd  $N = Z$  nucleus  $^{66}\text{As}$  [15]. Our analysis showed that there are essentially two different types of isomer entering into the discussion. One of them is shape isomer that occurs because prolate and oblate shapes can coexist at low excitations along the  $N = Z$  line. In fact, the prolate-oblate shape coexistence is a well known phenomenon in the neighboring even-even  $N = Z$  nucleus  $^{68}\text{Se}$  [16], where the ground state and the first excited state have oblate and prolate deformation, respectively [17, 18]. The first excited  $0^+$  state, which typically lies about several hundred keV above the ground state, can decay to the ground state via an electric monopole (E0) transition [19]. The E0 transition is a very slow process, and therefore, the first excited state becomes a shape isomer [7, 20]. Thus, we may expect that the low-spin  $7^+$  state in  $^{94}\text{Ag}$  is a shape isomer in nature.

The  $g_{9/2}$ -shell nuclei were extensively studied in the early years by the empirical shell model calculations [21, 22]. The very restricted model space ( $1p_{1/2}, 0g_{9/2}$ ) was used as it allowed an empirical fit for both residual interaction and single-particle energies. Herndl and Brown [23] performed a detailed study of the  $\beta$ -decay properties using the same model space. The interaction generally yielded a good agreement with experimental data of the high-spin spectroscopy. Later, the shell-model calculations with the  $fpg$  model space comprising the ( $1p_{3/2}, 0f_{5/2}, 1p_{1/2}, 0g_{9/2}$ ) shells together with a realistic interaction were performed [24]. The realistic effective interaction can in principle be derived from the free nucleon-nucleon interaction, and in fact, such microscopic interactions have been proposed for the beginning of the shell [25, 26]. However, these interactions failed to reproduce excitation spectra, binding energies, and transitions if many valence nucleons are considered. To overcome this defect, considerable effort has been put forward with an empirical fit to experimental data [27, 28].

On the other hand, realistic effective interactions are dominated by pairing and multipole interactions with the monopole term [29]. As documented in the literature, it has been shown that the extended  $P + QQ$  model works well for a wide range of  $N \approx Z$  nuclei [30, 31]. This model has demonstrated its capability of describing the microscopic structure in different nuclei, as for instance, in the  $fp$ -shell region [30] and the  $fpg$ -shell region [31].

In this paper, we perform the spherical large-scale shell model calculations in the  $fpg$  model space for the upper  $g_{9/2}$ -shell nuclei close to  $N = Z$  line. The structure of the isomeric states in the odd-odd  $N = Z$  nucleus  $^{94}\text{Ag}$  is investigated in detail. In particular, it is very interesting to study the deformation property of the high-spin  $21^+$  isomer. Our analysis shows that there are essentially two different types of isomer entering into the discussion. Due to the fact that prolate and oblate shapes can coexist at the low excitation region, a shape isomer is suggested for the low-spin  $7^+$  state in  $^{94}\text{Ag}$ . In an agreement with

the previous conclusion, the high-spin  $21^+$  isomer is interpreted as a spin-gap isomer. The spherical large-scale shell model calculations in the  $gds$  model space comprising the ( $0g_{9/2}, 1d_{5/2}, 0g_{7/2}, 2s_{1/2}$ ) shells are carried out to study the role of core excitations in the shell-model structure associated with a  $21^+ - 19^+$  level inversion in  $^{94}\text{Ag}$ .

The paper is arranged as follows. In Sec. II, we outline our model. In Section III, the shell model results are presented for several upper  $g_{9/2}$ -shell nuclei. In Section IV, we perform the numerical calculations and discuss the results for  $^{94}\text{Ag}$ . Finally, conclusions are drawn in Section V.

## II. THE MODEL

We start with the following form of Hamiltonian, which consists of pairing and multipole terms with the monopole interaction

$$\begin{aligned}
 H &= H_{\text{sp}} + H_{P_0} + H_{P_2} + H_{QQ} + H_{OO} + H_{\pi\nu}^{T=0} + H_{\text{mc}} \\
 &= \sum_{\alpha} \varepsilon_{\alpha} c_{\alpha}^{\dagger} c_{\alpha} - \sum_{J=0,2} \frac{1}{2} g_J \sum_{M\kappa} P_{JM1\kappa}^{\dagger} P_{JM1\kappa} \\
 &\quad - \frac{1}{2} \chi_2 / b^4 \sum_M : Q_{2M}^{\dagger} Q_{2M} : - \frac{1}{2} \chi_3 / b^6 \sum_M : O_{3M}^{\dagger} O_{3M} : \\
 &\quad - k^0 \sum_{a \leq b} \sum_{JM} A_{JM00}^{\dagger}(ab) A_{JM00}(ab) \\
 &\quad + \sum_{a \leq b} \sum_T k_{\text{mc}}^T(ab) \sum_{JMK} A_{JMTK}^{\dagger}(ab) A_{JMTK}(ab), \quad (1)
 \end{aligned}$$

where  $b$  in the third and fourth terms is the length parameter of harmonic oscillator. We take the  $J = 0$  and  $J = 2$  forces in the pairing channel, and the quadrupole-quadrupole ( $QQ$ ) and octupole-octupole ( $OO$ ) forces in the particle-hole channel [30, 31]. The monopole interaction is divided into two parts, namely the average  $T = 0$  monopole field  $H_{\pi\nu}^{T=0}$  and the monopole correction term  $H_{\text{mc}}$ . The Hamiltonian (1) is isospin invariant, and is diagonalized in a chosen model space based on a spherical basis [32]. In the present work, we first employ the  $fpg$  model space. This shell model has proven to be rather successful in describing energy levels and electromagnetic transitions. For the upper  $g_{9/2}$ -shell nuclei, we employ the single-particle energies  $\varepsilon_{p3/2} = 0.00$ ,  $\varepsilon_{f5/2} = 0.77$ ,  $\varepsilon_{p1/2} = 1.11$ , and  $\varepsilon_{g9/2} = 3.70$  (all in MeV). We adopt the following interaction strengths for the pairing and multipole forces

$$\begin{aligned}
 g_0 &= 24.0/A, \quad g_2 = 225.3/A^{5/3}, \\
 \chi_2 &= 480.0/A^{5/3}, \quad \chi_3 = 368.6/A^2 \text{ (in MeV)}, \quad (2)
 \end{aligned}$$

and for the monopole terms

$$\begin{aligned}
k_{\text{mc}}^{T=0}(a, g_{9/2}) &= -0.20 \text{ MeV}, & a = p_{3/2}, f_{5/2}, p_{1/2}, \\
k_{\text{mc}}^{T=1}(p_{3/2}, f_{5/2}) &= -0.3, & k_{\text{mc}}^{T=1}(p_{3/2}, p_{1/2}) = -0.3, \\
k_{\text{mc}}^{T=1}(f_{5/2}, p_{1/2}) &= -0.4, & k_{\text{mc}}^{T=1}(g_{9/2}, g_{9/2}) = -0.1, \\
k_{\text{mc}}^{T=0}(g_{9/2}, g_{9/2}) &= -0.75 \quad (\text{in MeV}). & (3)
\end{aligned}$$

We employ all the monopole terms used in our previous paper [33], with additional terms  $k_{\text{mc}}^{T=0}(a, g_{9/2})$  and  $k_{\text{mc}}^{T=0}(g_{9/2}, g_{9/2})$  [15]. These terms were found necessary for obtaining correct positions of the  $9_1^+$  and higher spin states relative to the  $7_1^+$  state in  $^{66}\text{As}$ . We have increased the strength of the monopole term  $k_{\text{mc}}^{T=0}(g_{9/2}, g_{9/2})$ , which gives effects of lowering the  $g_{9/2}$  orbital and the negative parity states. The  $T = 0$  monopole field  $H_{\pi\nu}^{T=0}$  affects significantly the relative energy between the  $T = 1$  and  $T = 0$  states in odd-odd  $N = Z$  nuclei [34]. We have determined the strength  $k^0$  to be  $64/A$  so as to reproduce the  $7^+$  state at the excitation energy 0.66 MeV in  $^{94}\text{Ag}$ . For calculations of spectroscopic  $Q$ -moments and  $B(E2)$  values, we use the standard effective charge  $e_\pi = 1.5e$  for protons and  $e_\nu = 0.5e$  for neutrons.

### III. CALCULATION OF UPPER $g_{9/2}$ -SHELL NUCLEI IN THE $fp_g$ MODEL SPACE

Before studying the odd-odd  $N = Z$  nucleus  $^{94}\text{Ag}$ , we first perform large-scale shell model calculations for several neighboring  $g_{9/2}$ -shell nuclei to validate our model. The calculations are carried out in the  $fp_g$  model space. The nuclei studied in this section are the heaviest  $N \approx Z$  nuclei for which energy levels could be obtained experimentally. The structure information of these nuclei is useful for the reaction network calculations of the rp process.

Figure 1 shows the energy levels for the Tc isotopes. As one can see, the calculated results reproduce satisfactorily the experimental levels for both even and odd parity observed in the odd-even nuclei  $^{91,93}\text{Tc}$ , and in the odd-odd nucleus  $^{92}\text{Tc}$ .

Comparison of the calculated energy levels with experimental data for the Ru isotopes are shown in Fig. 2 for even-even nuclei, and in Fig. 3 for odd-mass nuclei. Again, a good agreement with experimental data is achieved. In Ref. [34], some  $N \approx Z$  Ru isotopes were investigated by using a slightly different parameter set. Those calculations indicated an enhancement of quadrupole correlations in the  $N = Z$  nucleus  $^{88}\text{Ru}$ ; however the amount of the enhancement was not enough when compared the calculated moments of inertia with the experimental values. It was suggested that the  $1d_{5/2}$  orbital in the next major shell contributes very much to the quadrupole correlations. In fact, the moment of inertia can be easily reproduced with the truncated model space  $(1p_{1/2}, 0g_{9/2}, 1d_{5/2})$  that includes the  $1d_{5/2}$  orbital.

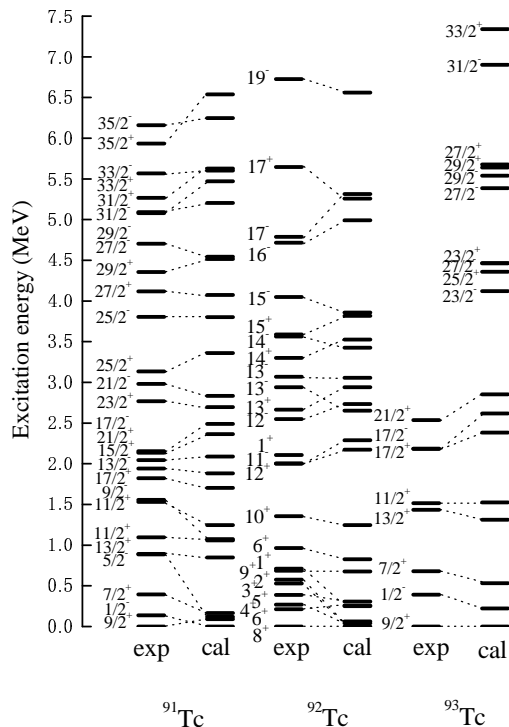


FIG. 1: Experimental and calculated energy levels of the odd-even nuclei  $^{91}\text{Tc}$ ,  $^{92}\text{Tc}$ , and  $^{93}\text{Tc}$ .

As we shall see in the next section, contribution from the  $1d_{5/2}$  orbital plays an important role also in  $^{94}\text{Ag}$ .

Fig. 4 shows the calculated energy levels for the odd-odd Rh isotopes  $^{90,92,94}\text{Rh}$ , and Fig. 5 for the odd-even  $^{93,95}\text{Rh}$ . The results are compared with experimental data if available. While the experimental levels of  $^{92,93}\text{Rh}$  are correctly reproduced and the  $^{95}\text{Rh}$  data are too sparse to allow a definite conclusion, our theoretical results for  $^{94}\text{Rh}$  are not in good agreement with data. This disagreement might indicate the importance of core excitation across the neutron shell-closure  $N = 50$  for this isotope, which is not taken into account in the present model space. Currently, there is no experimental information for the odd-odd  $N = Z$  nucleus  $^{90}\text{Rh}$ . Our calculation thus serves as a prediction, for the ground-state band with isospin  $T = 1$  and a side band with  $T = 0$ . It is interesting to mention that from our calculation, the spectroscopic quadrupole moments are negative in the ground-state band, while those in the side band are positive, except for the  $7^+$  state at an excitation about 1 MeV. Therefore, we suggest that both the  $T = 0$  band-head  $1^+$  state and the low-lying  $7^+$  state may be considered as a candidate of shape isomer.

In Figs. 6 and 7, theoretical energy levels of the Pd isotopes are compared with experiment. According to Ref. [4],  $^{92,93}\text{Pd}$  are waiting point nuclei and their structure information is important for the rp process nucleosynthesis. As one can see from Figs. 6 and 7, all the known energy levels for both even-even and even-odd isotopes are well reproduced. It has been confirmed experimen-

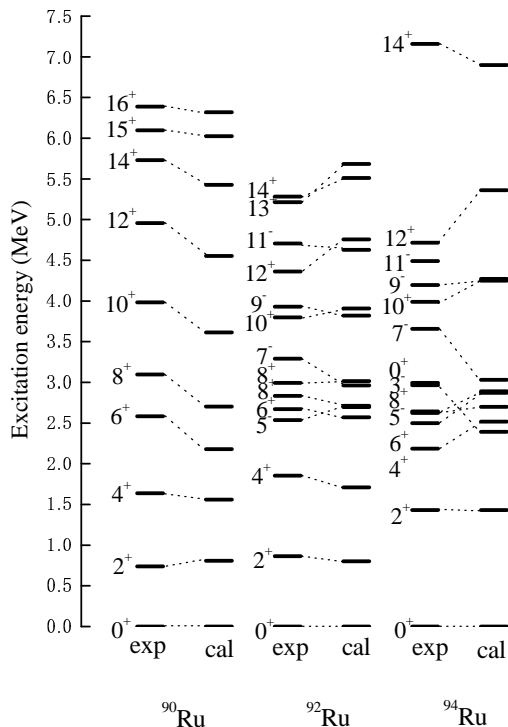


FIG. 2: Experimental and calculated energy levels of the even-even nuclei  $^{90}\text{Ru}$ ,  $^{92}\text{Ru}$ , and  $^{94}\text{Ru}$ .

tally that the  $14^+$  state in  $^{94}\text{Pd}$  is an isomer [2]. Using the standard effective charges  $1.5e$  for protons and  $0.5e$  for neutrons, we have obtained  $B(E2; 14^+ \rightarrow 12^+) = 39.6 e^2 fm^4$  for the isomeric  $14^+$  state. This value is very close to the experimental estimate  $B(E2) = 44(6) e^2 fm^4$  or  $B(E2) = 39(9) e^2 fm^4$ . In Fig. 7, our calculation predicts a low-lying  $11/2^+$  level in  $^{93}\text{Pd}$  which has not been seen experimentally. The theoretical level scheme for  $^{95}\text{Pd}$  correctly gives a  $21/2^+$  isomeric state that is de-excited by an  $E4$  decay. No experimental information is currently available for the even-even  $N = Z$  nucleus  $^{92}\text{Pd}$ . The level scheme for  $^{92}\text{Pd}$  is thus our prediction, where the calculated ground-state band and the side band are suggested to have isospin  $T = 1$  and  $T = 0$ , respectively.

Figure 8 shows the theoretical level scheme of the odd-odd  $N = Z$  nucleus  $^{94}\text{Ag}$  calculated within the present model space, together with that obtained with the *slgt0* effective interaction for the  $(1p_{1/2}, 0g_{9/2})$  model space. The experimentally known isomers in this nucleus include the low-spin  $7^+$  and the high-spin  $21^+$  one. The question why these states become isomeric has, in our opinion, not been thoroughly addressed. The excitation energy, spin, and parity of the  $7^+$  isomer have not been determined experimentally. In the present calculation, we obtain a  $7^+$  state around the excitation energy 0.66 MeV, which only has the  $0^+$  ground state and the  $1^+$  state below it. Therefore, decay out from the  $7^+$  state can be strongly hindered by the selection rule. This already creates a favorable condition for the  $7^+$  state to

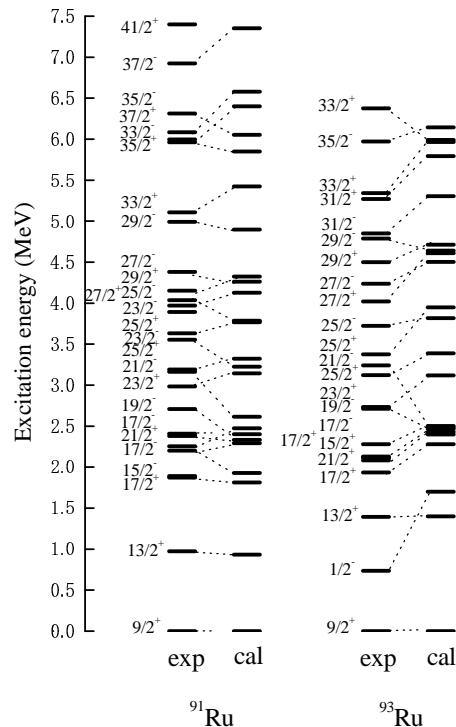


FIG. 3: Experimental and calculated energy levels of the even-odd nuclei  $^{91}\text{Ru}$ , and  $^{93}\text{Ru}$ .

be isomeric. In Table I, we further analyze the structure of the isomeric state by showing expectation values of nucleon number in four orbitals as well as calculated spectroscopic quadrupole moments. It is interesting to note that the results indicate a very different structure of the  $7^+$  state from the neighboring states of  $1^+$ ,  $3^+$  and  $5^+$ . Opposite to all those neighboring states, the  $7^+$  state takes a quadrupole moment with positive value. Hence the shape of the  $7^+$  state is predicted to be oblate, in contrast to the prolate shape for other neighboring states. In this sense, the  $7^+$  state can be considered to be a shape isomer.

Calculated energy levels for the odd-mass nucleus  $^{95}\text{Ag}$  are shown in Fig. 9. The calculation has well reproduced the known experimental levels in the low-spin part while the theoretical levels of the high spin states are too high as compared to data. The calculation produces a level inversion in which the  $23/2^+$  state lies below the  $21/2^+$  state. Thus, decay of the  $23/2^+$  level has to go with an  $E4/M3$  transition. This may suggest a possible isomerism of the  $23/2^+$  state. However, our calculation cannot explain the experimental finding that the  $23/2^+$  state decays to the  $17/2^-$  one through an  $E3$  transition.

Finally, theoretical energy levels of the Cd isotopes are shown in Fig. 10. The experimentally known energy levels for  $^{98}\text{Cd}$  are well reproduced. In recent experiment [35], the  $12^+$  isomer was identified at 6.635 MeV in  $^{98}\text{Cd}$ . In the present calculations, however, the  $12^+$  state is out of the *fp**g* shell configurations and the upper shells such as  $1d_{5/2}$  orbital are needed. For the even-even  $N = Z$

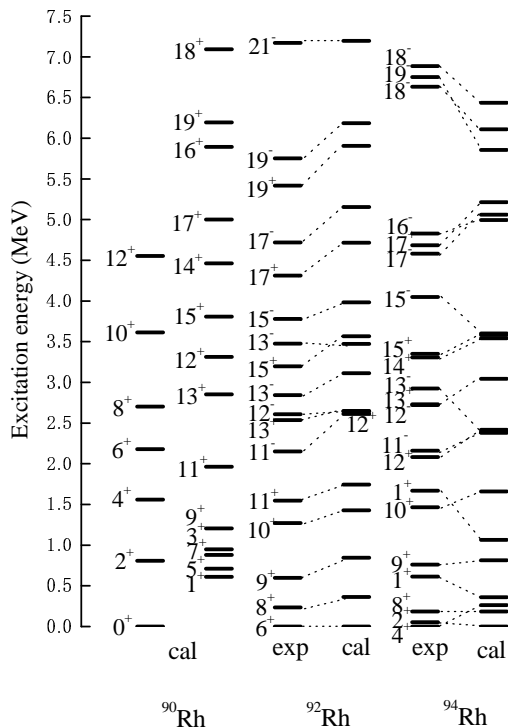


FIG. 4: Experimental and calculated energy levels of the odd-odd nuclei  $^{90}\text{Rh}$ ,  $^{92}\text{Rh}$ , and  $^{94}\text{Rh}$ .

nucleus  $^{96}\text{Cd}$ , which has not been investigated experimentally, our model yields the ground and side bands as shown in Fig. 10. It is worthwhile to mention that the present calculation predicts a spin-gap isomer with spin-parity  $16^+$  at about 5.2 MeV, in consistent with the shell model result obtained in the restricted  $(1p_{1/2}, 0g_{9/2})$  model space.  $^{96}\text{Cd}$  is known as a waiting point nucleus [4].

TABLE I: Expectation values of proton or neutron numbers occupied in the four orbitals, calculated for the low-lying  $T = 0$  states of  $I^\pi$  in the  $fp_g$ -shell model space. Calculated spectroscopic  $Q$ -moments (in  $e\text{ fm}^2$ ) are also tabulated.

$^{94}\text{Ag}$	$p_{3/2}$	$f_{5/2}$	$p_{1/2}$	$g_{9/2}$	$Q$
$1_1^+$	3.93	5.97	1.99	7.11	-16.6
$3_1^+$	3.93	5.97	2.00	7.10	-29.6
$5_1^+$	3.95	5.97	1.99	7.09	-26.7
$7_1^+$	3.95	5.96	2.00	7.08	61.2
$9_1^+$	3.98	5.95	1.99	7.08	23.8
$11_1^+$	3.56	5.92	1.98	7.66	44.5
$13_1^+$	3.75	5.77	1.91	7.57	55.0
$15_1^+$	3.98	5.44	1.98	7.60	55.2
$17_1^+$	3.83	5.68	1.96	7.52	43.6
$19_1^+$	3.82	5.72	1.95	7.51	48.3
$21_1^+$	4.00	5.50	2.00	7.50	57.7

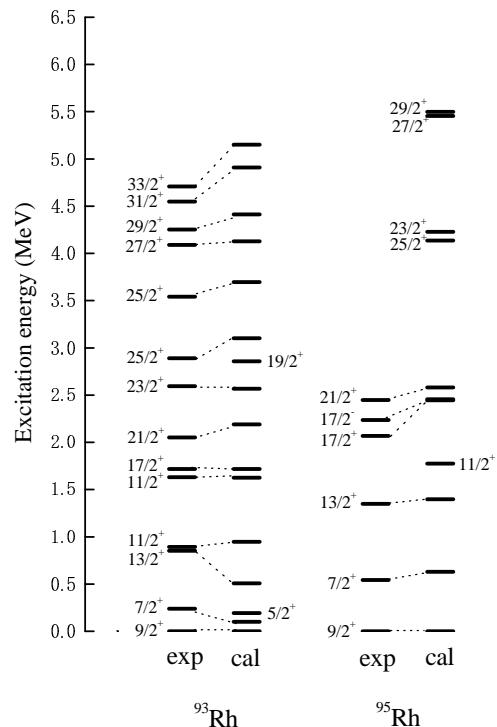


FIG. 5: Experimental and calculated energy levels of the odd-even nuclei  $^{93}\text{Rh}$  and  $^{95}\text{Rh}$ .

#### IV. CALCULATION WITH THE $gds$ MODEL SPACE FOR $^{94}\text{Ag}$

We have demonstrated the power of our  $fp_g$  shell model in a systematical description of proton-rich upper  $g_{9/2}$ -shell nuclei. For  $^{94}\text{Ag}$ , the model has explained the structure of the low-lying isomer  $7^+$ . The calculation with this  $(1p_{3/2}, 0f_{5/2}, 1p_{1/2}, 0g_{9/2})$  model space, however, could not reproduce the high-spin isomer  $21^+$  in  $^{94}\text{Ag}$ . It gives a quite large electric quadrupole transition value,  $B(E2; 21^+ \rightarrow 19^+) = 58.9 e^2\text{fm}^4$ , which corresponds to a fast decay to the lower state  $19^+$ . This result is similar to that obtained in the shell model calculation with the restricted  $(1p_{1/2}, 0g_{9/2})$  model space [22]. On the other hand, it has recently been reported by Plettner *et al.* [9] that the shell model calculation in the  $(0g_{9/2}, 1d_{5/2}, 0g_{7/2}, 1d_{3/2}, 2s_{1/2})$  model space can predict the isomerism of the  $21^+$  state due to a  $21^+$ - $19^+$  level inversion. The work of Plettner *et al.* thus suggests an important contribution from the upper orbitals above  $0g_{9/2}$ .

In a previous paper [34] that discusses the structure of the even-even  $N = Z$  nucleus  $^{88}\text{Ru}$ , some of us suggested that the  $1d_{5/2}$  orbit above the  $fp_g$ -shell plays a significant role in the collectivity of that nucleus. The  $1d_{5/2}$  orbit is expected to contribute to the quadrupole correlation because it couples strongly with the  $0g_{9/2}$  orbit through the  $Q$  matrix element  $\langle 0g_{9/2} || Q || 1d_{5/2} \rangle$  with  $\Delta l = \Delta j = 2$ . Simply adding the  $1d_{5/2}$  orbit to the current model space  $(1p_{3/2}, 0f_{5/2}, 1p_{1/2}, 0g_{9/2})$ , unfortunately, makes the con-

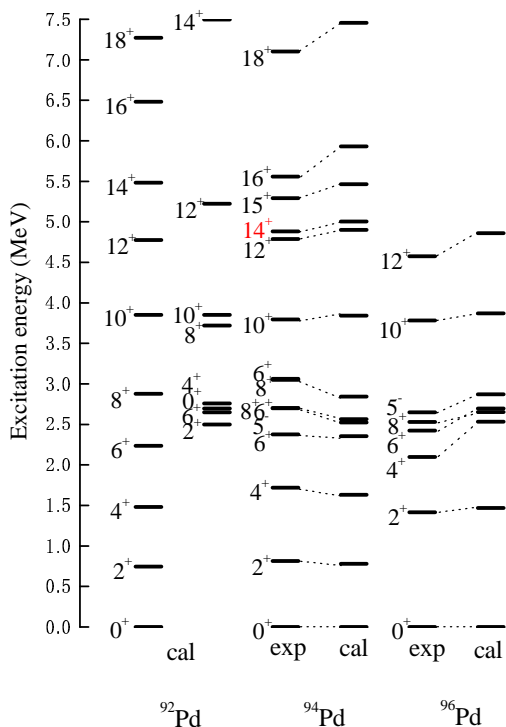


FIG. 6: (Color online) Experimental and calculated energy levels with  $T = 1$  of the even-even nuclei  $^{92}\text{Pd}$ ,  $^{94}\text{Pd}$ , and  $^{96}\text{Pd}$ .

figuration space too large. In order to include the  $1d_{5/2}$  orbit, we have to truncate out some lower orbits that may not be very important for the present discussion. Table I has shown that for the upper  $g_{9/2}$ -shell nuclei, the contribution from the  $(1p_{3/2}, 0f_{5/2}, 1p_{1/2})$  shells is not so large as compared to the  $0g_{9/2}$  orbit. Accordingly, we shall examine the contribution of the  $1d_{5/2}$  orbit within the truncated space  $(0g_{9/2}, 1d_{5/2}, 0g_{7/2}, 2s_{1/2})$ , hereafter called the  $gds$  model space. This model space, without  $(1p_{3/2}, 0f_{5/2}, 1p_{1/2})$ , is expected to work properly as it can explain the main features of the upper  $g_{9/2}$ -shell nuclei [36, 37].

Let us now perform large-scale shell model calculations within the  $gds$  model space, which allows excitations across the  $N = Z = 50$  shell gap. For the single-particle energies, we employ the predicted ones from the global fit of all available single-particle and single-hole energies [38, 39] of Duflo and Zuker [40], i.e.,  $\varepsilon_{g_{9/2}} = 0.0$ ,  $\varepsilon_{d_{5/2}} = 2.54$ ,  $\varepsilon_{g_{7/2}} = 4.95$ , and  $\varepsilon_{s_{1/2}} = 3.34$  in MeV. For the interaction strengths in the Hamiltonian, the following constants are adopted as

$$\begin{aligned} g_0 &= 24.0/A, & g_2 &= 225.3/A^{5/3}, \\ \chi_2 &= 240.0/A^{5/3} \text{ in MeV.} \end{aligned} \quad (4)$$

The octupole-octupole force and the monopole correction terms are neglected because without these terms, the essential feature of level sequences does not change. The inclusion of  $1d_{5/2}$  orbit allows us to use a weaker quadrupole force, and therefore,  $\chi_2$  in (4) is smaller than

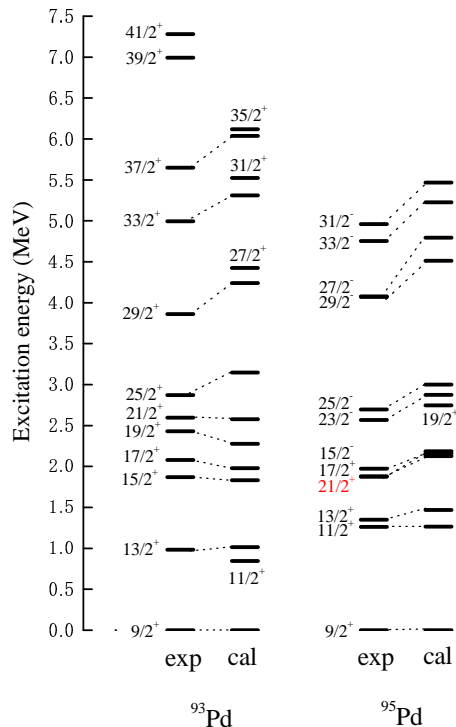


FIG. 7: (Color online) Experimental and calculated energy levels of the even-odd nuclei  $^{93}\text{Pd}$  and  $^{95}\text{Pd}$ .

that in Eq. (2). It is interesting to note that these force strengths are close to those employed in our previous paper [15]. The  $T = 0$  monopole field  $H_{\pi\nu}^{T=0}$  influences strongly the relative energy between the  $T = 1$  and  $T = 0$  states in odd-odd  $N = Z$  nuclei [34]. The strength  $k^0 = 64/A$  is chosen so as to reproduce the excitation energy 0.66 MeV of the low-lying  $7^+$  state. Again, we take the standard effective charges  $e_\pi = 1.5e$  for protons and  $e_\nu = 0.5e$  for neutrons.

Calculations are performed by allowing up to 3p-3h excitations across the  $N = Z = 50$  shell gap, which are sufficient for the present discussion. Energy levels of  $^{94}\text{Ag}$  obtained from this calculation are shown in Fig. 11. Results from different model spaces are also given for comparison. As one can see, the three results are quite similar, and they all reproduce well the few known experimental energy levels. The closely-lying  $12^+$  and  $14^+$  states with  $T = 1$  may well correspond to those discussed in  $^{94}\text{Pd}$  (see Fig. 6). However, one clear difference among the three results is that the  $gds$ -shell model calculation yields a  $21^+$ - $19^+$  level inversion, with the  $19^+$  level lying 25.7 keV above the  $21^+$  level. The calculated E4 transition probability  $B(E4; 21^+ \rightarrow 17^+)$  is very small. We can thus explain the isomeric nature of the  $21^+$  state within the  $gds$  shell model, in accordance with the result of Pletner *et al.* [9] in the  $(0g_{9/2}, 1d_{5/2}, 0g_{7/2}, 2s_{1/2}, 1d_{3/2})$  model space. We mention that there is an interesting precedent, the  $12^+$  isomer in  $^{52}\text{Fe}$ . As already noted in Ref. [27], this phenomenon is due to jumps from the  $f_{7/2}$  orbital to the above  $f_p$ -shell. Similarly, we can consider that the

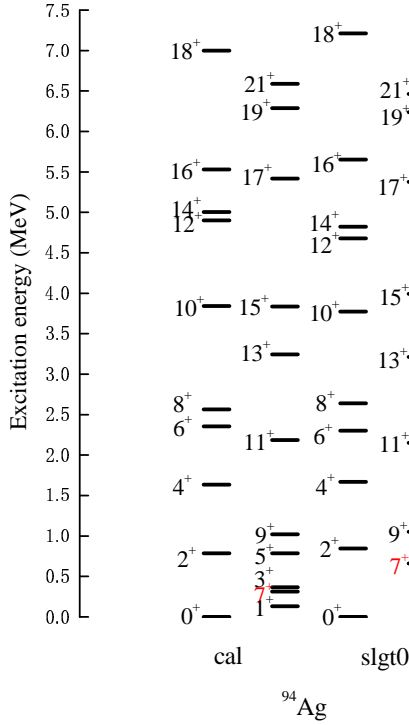


FIG. 8: (Color online) Energy levels of the odd-odd  $N = Z$  nucleus  $^{94}\text{Ag}$  for the extended  $P + QQ$  force in the  $fpg$ -shell and the  $slg0$  interaction in the restricted  $(p_{1/2}, g_{9/2})$  model space.

$21^+$  isomerism is due to jumps from the  $g_{9/2}$  orbital to the above  $sdg$ -shell.

Excitation energies of the  $T = 0$  states are plotted as functions of total spin  $I$  in Fig. 12. The figure displays an approximate linear dependence of excitation energy on the total spin  $I$ , with a clear deviation of the  $21^+$  state from the straight line. Thus, our shell model calculations demonstrate the importance of excitations across the  $^{100}\text{Sn}$  closed shell, which causes a  $21^+$ - $19^+$  level inversion, and hence the  $21^+$  isomerism.

With our shell model results, we now further examine the microscopic structure of the isomeric  $7^+$  and  $21^+$  states in  $^{94}\text{Ag}$ . In Table II, we present the expectation values of particle numbers in four orbitals, calculated for the low-lying  $T = 0$  states in  $^{94}\text{Ag}$ . Theoretical spectroscopic  $Q$ -moments (in  $e \text{ fm}^2$ ) are also included in the table. To be better visualized, these occupation numbers are plotted as functions of total spin  $I$  in Fig. 13, where for the  $0g_{9/2}$  orbital, the plotted numbers are 0.1 times of their actual values. The results show that the most occupied orbit is  $0g_{9/2}$ . The occupation number of the  $1d_{5/2}$  orbit is 0.43 for the  $7^+$  state. With increasing  $I$ , it decreases linearly, but begins to rise at  $21^+$ . For the high-spin states  $23^+$  and  $25^+$ , a drastic increase of  $1d_{5/2}$  occupation is observed. The  $21^+$  state has the maximum aligned hole configurations in the  $fpg$  shell for neutrons and protons, which coupled strongly with the  $1d_{5/2}$  configurations. The extra binding energy due to the large

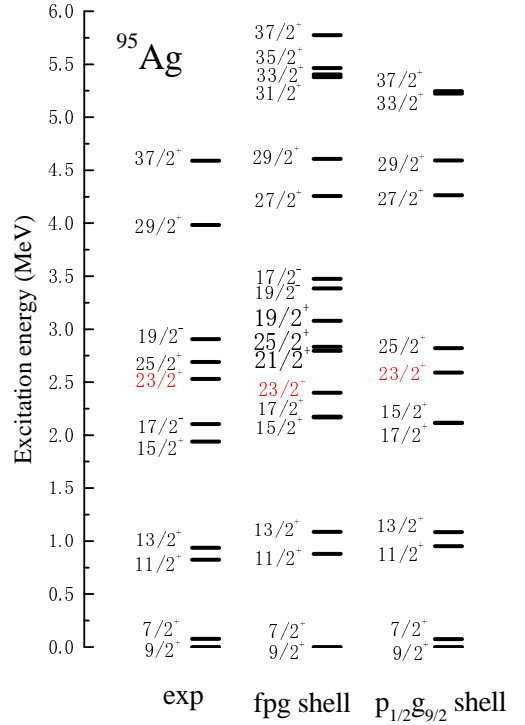


FIG. 9: (Color online) Experimental and calculated energy levels of  $^{95}\text{Ag}$  in the  $fpg$ -shell and the  $(p_{1/2}, g_{9/2})$  model space.

attractive  $pn$  interaction in the  $0g_{9/2}$  orbit lowers the  $21^+$  state primarily. However, this is not sufficient to make the  $21^+$  state isomeric. It is the mixing with the  $1d_{5/2}$  configurations that eventually causes the  $21^+$ - $19^+$  level inversion so that the  $21^+$  state becomes an isomer.

In Fig. 14, we plot the two calculations of spectroscopic  $Q$ -moments for the  $T = 0$  excited states as a function of total spin  $I$ , using the numbers listed in Tables

TABLE II: Expectation values of proton or neutron numbers occupied in the four orbitals, calculated for the low-lying  $T = 0$  states of  $I^\pi$  in the  $gds$ -shell model space. Calculated spectroscopic  $Q$ -moments (in  $e \text{ fm}^2$ ) are also tabulated.

$^{94}\text{Ag}$	$g_{9/2}$	$d_{5/2}$	$g_{7/2}$	$s_{1/2}$	$Q$
$1_1^+$	6.50	0.43	0.04	0.03	-30.7
$3_1^+$	6.51	0.43	0.04	0.03	-52.0
$5_1^+$	6.52	0.41	0.04	0.03	-53.2
$7_1^+$	6.51	0.43	0.04	0.03	109.6
$9_1^+$	6.55	0.38	0.04	0.03	43.0
$11_1^+$	6.56	0.37	0.04	0.03	11.1
$13_1^+$	6.62	0.32	0.04	0.02	9.2
$15_1^+$	6.65	0.29	0.04	0.02	70.5
$17_1^+$	6.70	0.26	0.03	0.02	39.3
$19_1^+$	6.72	0.23	0.03	0.02	53.3
$21_1^+$	6.70	0.26	0.03	0.02	84.1

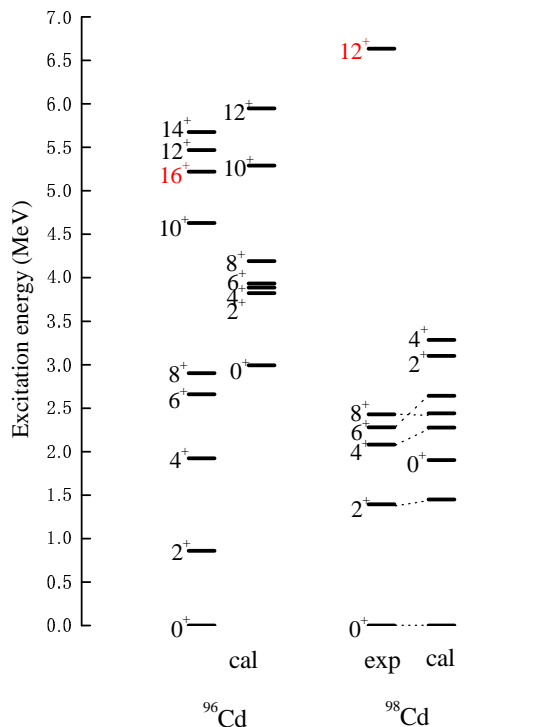


FIG. 10: (Color online) Experimental and calculated energy levels of the even-even nuclei  $^{96}\text{Cd}$  and  $^{98}\text{Cd}$ .

I and II. Comparing the *fpg*-shell and *gds*-shell model calculations, one sees a clear enhancement in  $Q$ -moment at the  $7^+$ ,  $15^+$ , and  $21^+$  states due to the excitations across the  $^{100}\text{Sn}$  shell-closure. We thus conclude that the inclusion of the  $1d_{5/2}$  orbit enhances significantly the collectivity of the isomeric  $7^+$  and  $21^+$  states. In the *gds*-shell calculation, the spectroscopic  $Q$ -moments for  $7^+$  and  $21^+$  states are predicted to be  $109.6 e \text{ fm}^2$  and  $84.1 e \text{ fm}^2$ , respectively.

The above conclusion is further supported by  $B(E2)$  calculations shown in Table III. There, the  $B(E2)$  values are presented along the two decay sequences with  $T = 0$  and  $T = 1$ . What we can learn from the table is the fact that the numbers in the column of the *gds*-shell calculation are always larger than those of the *fpg*-shell results. This indicates that the core excitations across the  $N = Z = 50$  shell gap increase the  $B(E2)$  values, which is consistent with the observation in Fig. 14. Moreover, the transition  $B(E2, 7^+ \rightarrow 5^+)$  is very small also in the *gds*-shell calculation, implying that the core excitation does not wash out the isomeric nature of the  $7^+$  state as discussed in the *fpg*-shell calculation.

The analysis on one- and two-proton decay of the  $21^+$  isomer has suggested a large deformation for this state. Mukha *et al.* [13] argued that the unexpectedly large probability for the proton decay is attributed to a large prolate shape of the parent nucleus. We note that shape is a widely-used concept but not a direct shell model consequence. In order to discuss shapes using the present shell model results, assumptions are needed. By assum-

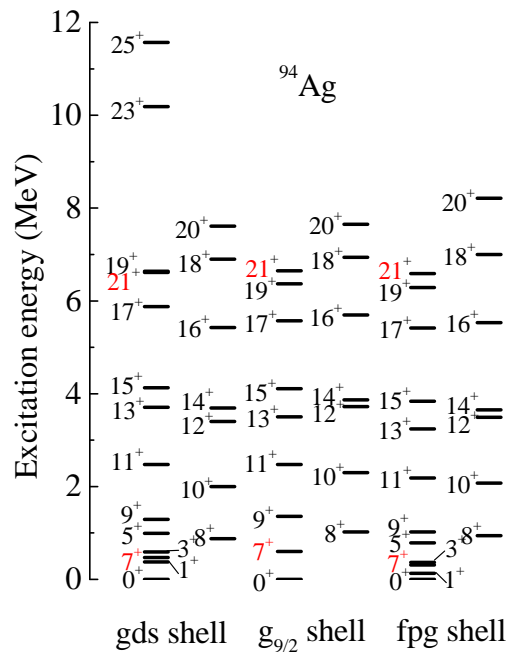


FIG. 11: (Color online) Calculated energy levels with  $T = 0$  of the odd-odd  $N = Z$  nucleus  $^{94}\text{Ag}$  with the *gds*-shell,  $g_{9/2}$ -shell, and *fpg*-shell model spaces.

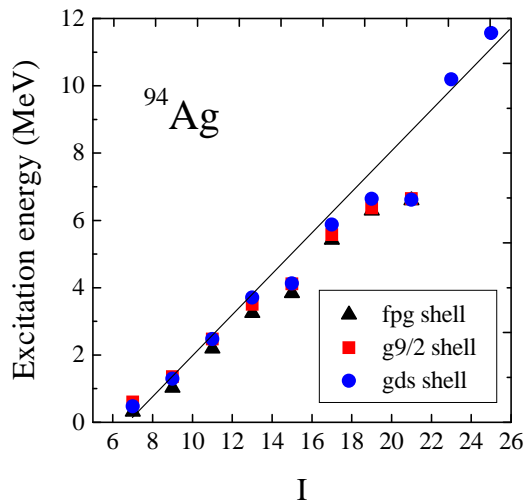


FIG. 12: (Color online) Excitation energies of the  $T = 0$  states in  $^{94}\text{Ag}$  from the *gds*-shell,  $g_{9/2}$ -shell, and *fpg*-shell model calculations. The diagonal line is a linear fit.

ing an axial symmetric rotor for  $^{94}\text{Ag}$ , deformations for the isomeric  $7^+$  and  $21^+$  states can be estimated to be  $\beta = -0.5$  and  $\beta = -0.2$  from the spectroscopic  $Q$ -moments  $109.6 e \text{ fm}^2$  and  $84.1 e \text{ fm}^2$ , respectively, if a  $K = 0$  is further assumed for both states. While the assumption of  $K = 0$  may be reasonable for the  $7^+$  state, it leads to a conclusion that the  $21^+$  state corresponds to an oblate shape, in contradiction to the conclusion of Ref. [13]. However, a prolate shape of  $\beta = +0.2$  can be obtained if, for example, a  $K = 21$  is assumed for the



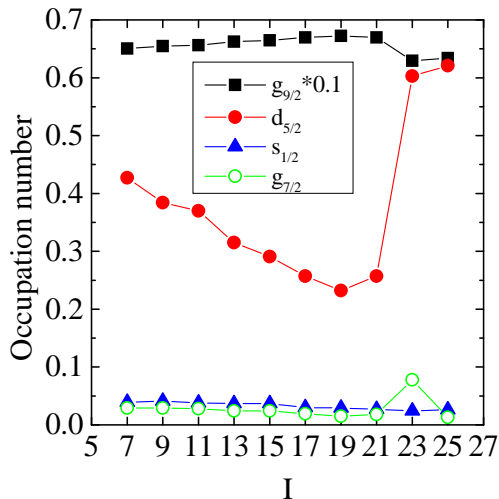


FIG. 13: (Color online) Calculated occupation number as a function of total spin in  $^{94}\text{Ag}$  for the  $gds$ -shell model calculations. The occupation numbers of  $0g_{9/2}$  orbital are plotted as 0.1 times of their actual values.

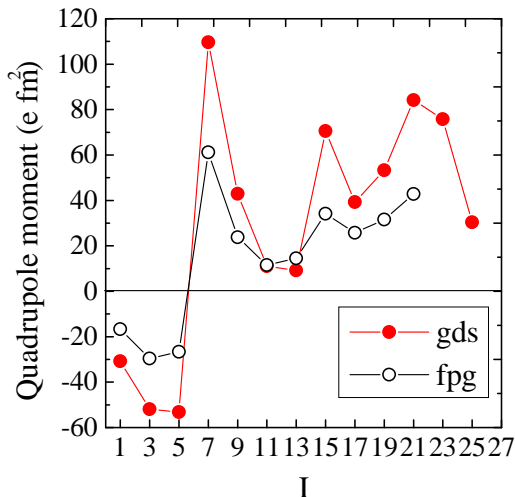


FIG. 14: (Color online) Spectroscopic quadrupole moments as a function of total spin.

$21^+$  state. The present calculations in the  $gds$ -shell do not show strong deformation. As suggested by I. Mukha *et al.* [12], the  $1h_{11/2}$  single-proton orbital may be important for a strongly deformed shape of the  $21^+$  isomer in  $^{94}\text{Ag}$ . Independent of these assumptions, a measurement of the laboratory quadrupole moments for the isomeric states, which may be compared directly to our theoretical results listed in Tables I and II, is desired.

## V. CONCLUSIONS

In this paper, we have investigated the microscopic structure of isomers in  $^{94}\text{Ag}$  within a large-scale shell model framework. To demonstrate that our model is re-

liable with predictive power, we have systematically calculated other nuclei in the same mass region, for all even-even, even-odd, odd-even, and odd-odd types of nuclei, and compared the results with available data. Overall, a good agreement has been obtained. For those  $N = Z$  nuclei (in addition to  $^{94}\text{Ag}$ , also  $^{90}\text{Rh}$ ,  $^{92}\text{Pd}$ , and  $^{96}\text{Cd}$ ) for which no experimental information is available, the calculations may serve as predictions for future experiment. In particular, the discussed structure for those waiting point nuclei may be useful for the reaction network calculations of the rp process nucleosynthesis.

We have shown that the isomerism of the  $7^+$  and  $21^+$  states in  $^{94}\text{Ag}$  is attributed to an enhancement of collectivity that causes large deformation. The isomeric  $7^+$  state has been suggested as a shape isomer because this isomerism is due to shape difference between this and the lower-lying states. The  $21^+$  isomer is produced by a different mechanism, namely, a level inversion of the  $19^+$  and  $21^+$  states from their normal order. We have found that this unusual level inversion is caused by excitations across the  $^{100}\text{Sn}$  shell closure to the upper shells including the  $1d_{5/2}$  orbital. This conclusion is in an agreement with the previous finding by Plettner *et al.* [9].

It was discussed by Mukha *et al.* [13] that the fine structure of the observed proton decay would require a large deformation for the  $21^+$  isomeric state, and the unexpectedly large probability for the observed two-proton decay could be attributed to a strongly deformed prolate shape in  $^{94}\text{Ag}$ . The present shell model calculation does not yield a large deformation for the  $21^+$  isomer, and it cannot provide a conclusive support for the claim about a definite shape because in order to link the shell model results to a geometric shape, one has to introduce

TABLE III:  $B(E2 : J_i \rightarrow J_f)$  for the  $T = 0$  and  $T = 1$  states of  $^{94}\text{Ag}$ .

$J_i \rightarrow J_f$	$B(E2 : J_i \rightarrow J_f)$ in $e^2\text{fm}^4$	
	$fpg$ -shell	$gds$ -shell
$T = 0$		
$3 \rightarrow 1$	474	669
$5 \rightarrow 3$	364	757
$7 \rightarrow 5$	0.0	0.26
$9 \rightarrow 7$	41	78
$11 \rightarrow 9$	139	298
$13 \rightarrow 11$	93	361
$15 \rightarrow 13$	63	88
$17 \rightarrow 15$	43	103
$19 \rightarrow 17$	103	130
$21 \rightarrow 19$	59	109
$T = 1$		
$2 \rightarrow 0$	193	497
$4 \rightarrow 2$	250	719
$6 \rightarrow 4$	247	718
$8 \rightarrow 6$	32	17

assumptions similar as those utilized in Ref. [13]. The present result indicating no huge deformation of  $^{94}\text{Ag}$  isomer could be reasonable because the ground states of nuclei in this region are very weakly deformed. It remains an open question of whether a more extended shell model space can obtain a large deformation. Our calculations predict that the  $21^+$  isomer has large positive value of

the spectroscopic  $Q$ -moment. To confirm this, the nuclear  $Q$ -moment should be measured directly.

Y.S. is supported by the Chinese Major State Basic Research Development Program through grant 2007CB815005, and by the the U. S. National Science Foundation through grant PHY-0216783.

- 
- [1] K. Ogawa, Phys. Rev. C **28**, 958 (1983).  
 [2] N. Marginean *et al.*, Phys. Rev. C **67**, 061301(R) (2003).  
 [3] L. Van Wormer *et al.*, Astrophys. J. **432**, 326 (1994).  
 [4] H. Schatz *et al.*, Phys. Rep. **294**, 167 (1998).  
 [5] H. Schatz *et al.*, Phys. Rev. Lett. **86**, 3471 (2001).  
 [6] A. Aprahamian and Y. Sun, Nature Phys. **1**, 81 (2005).  
 [7] Y. Sun, M. Wiescher, A. Aprahamian, and J. Fisker, Nucl. Phys. A **758**, 765 (2005).  
 [8] M. La Commara *et al.*, Nucl. Phys. A **708**, 167 (2002).  
 [9] C. Plettner *et al.*, Nucl. Phys. A **733**, 20 (2004).  
 [10] I. Mukha *et al.*, Phys. Rev. C **70**, 044311 (2004).  
 [11] I. Mukha *et al.*, Nucl. Phys. A **746**, 66c (2004).  
 [12] I. Mukha *et al.*, Phys. Rev. Lett. **95**, 022501 (2005).  
 [13] I. Mukha *et al.*, Nature **439**, 298 (2006).  
 [14] E. Roeckl *et al.*, ACTA PHYSICA POLONICA B **38**, 1121 (2007).  
 [15] M. Hasegawa, Y. Sun, K. Kaneko, and T. Mizusaki, Phys. Lett. B **617**, 150 (2005).  
 [16] S. M. Fischer *et al.*, Phys. Rev. Lett. **87**, 132501 (2001).  
 [17] K. Kaneko, M. Hasegawa, and T. Mizusaki, Phys. Rev. C **70** 051301(R) (2004).  
 [18] Y. Sun, Eur. Phys. J. A **20**, 133 (2004).  
 [19] E. Bouchez *et al.*, Phys. Rev. Lett. **90**, 082502 (2003).  
 [20] P. Walker and G. Dracoulis, Nature **399**, 35 (1999).  
 [21] R. Gross and A. Frenkel, Nucl. Phys. A **267**, 85 (1976).  
 [22] F. J. D. Serduke, R. D. Lawson, and D. H. Gloecker, Nucl. Phys. A **256**, 45 (1976).  
 [23] F. Herndel and B. A. Brown, Nucl. Phys. A **627**, 35 (1997).  
 [24] K. Schmidt *et al.*, Z. Phys. A **350**, 99 (1994).  
 [25] T. T. S. Kuo and G. E. Brown, Nucl. Phys. A **114**, 241 (1968).  
 [26] M. Hjorth-Jensen, T. T. S. Kuo, and E. Osnes, Phys. Repts. **261**, 125 (1995).  
 [27] A. Poves and A. P. Zuker, Phys. Rep. **70**, 235 (1981).  
 [28] M. Honma, T. Otsuka, B. A. Brown, and T. Mizusaki, Phys. Rev. C **69**, 034335 (2004).  
 [29] M. Dufour and A. P. Zuker, Phys. Rev. C **54**, 1641 (1996).  
 [30] M. Hasegawa, K. Kaneko, and S. Tazaki, Nucl. Phys. A **688** (2001) 765.  
 [31] K. Kaneko, M. Hasegawa, and T. Mizusaki, Phys. Rev. C **66** 051306(R) (2002).  
 [32] T. Mizusaki, RIKEN Accel. Prog. Rep. **33**, 14 (2000).  
 [33] M. Hasegawa, K. Kaneko, and T. Mizusaki, Phys. Rev. C **71**, 044301 (2005).  
 [34] M. Hasegawa, K. Kaneko, T. Mizusaki, and S. Tazaki, Phys. Rev. C **69**, 034324 (2004).  
 [35] A. Blazhev *et al.*, Phys. Rev. C **69**, 064304 (2004).  
 [36] A. P. Zuker, J. Retamosa, A. Poves, and E. Caurier, Phys. Rev. C **52**, R1741 (1995).  
 [37] E. Caurier *et al.*, in ENAM2001, Eur. Phys. J. A. **15**, 145 (2002).  
 [38] F. Nowacki *et al.*, Nucl. Phys. A **704**, 223c (2002).  
 [39] H. Grawe *et al.*, Nucl. Phys. A **704**, 211c (2002).  
 [40] J. Duflo and A. P. Zuker, Phys. Rev. C **59**, R2347 (1999).  
 [41] C. Rusu *et al.*, Phys. Rev. C **69**, 024307 (2004).